Published in final edited form as:
Cancer Res. 2014 December 1; 74(23): 7024–7036. doi:10.1158/0008-5472.CAN-14-1346.

Hedgehog signaling drives radioresistance and stroma-driven tumor repopulation in head and neck squamous cancers

Gregory N. Gan[1], **Justin Eagles**[2], **Stephen B. Keysar**[2], **Guoliang Wang**[2], **Magdalena J. Glogowska**[2], **Cem Altunbas**[1], **Ryan T. Anderson**[2], **Phuong N. Le**[2], **J. Jason Morton**[2], **Barbara Frederick**[1], **David Raben**[1], **Xiao-Jing Wang**[3,4], and **Antonio Jimeno**[2,4,5]

[1]Department of Radiation Oncology, University of Colorado School of Medicine, Aurora CO.

[2]Division of Medical Oncology, Department of Medicine, University of Colorado School of Medicine, Aurora CO.

[3]Department of Pathology, University of Colorado School of Medicine, Aurora CO.

[4]Charles C. Gates Center for Stem Cell Biology, University of Colorado School of Medicine, Aurora CO.

[5]Department of Otolaryngology, University of Colorado School of Medicine, Aurora CO.

Abstract

Local control and overall survival in patients with advanced head and neck squamous cell cancer (HNSCC) remains dismal. Signaling through the Hedgehog (Hh) pathway is associated with epithelial-to-mesenchymal transition (EMT) and activation of the Hh effector transcription factor Gli1 is a poor prognostic factor in this disease setting. Here we report that increased GLI1 expression in the leading edge of HNSCC tumors is further increased by irradition where it contributes to therapy resistance. Hh pathway blockade with cyclopamine suppressed GLI1 activation and enhanced tumor sensitivity to radiotherapy. Further, radiotherapy-induced GLI1 expression was mediated in part by the mTOR/S6K1 pathway. Stroma exposed to radiotherapy promoted rapid tumor repopulation and this effect was suppressed by Hh inhibition. Our results demonstrate that GLI1 is upregulated at the tumor-stroma intersection in HNSCC is elevated by radiotherapy where it contributes to stromal-mediated resistance, and that Hh inhibitors offer a rational strategy to reverse this process to sensitize HNSCC to radiotherapy.

Keywords

Head and neck squamous cell cancer; hedgehog pathway; radiotherapy; tumor repopulation; epithelial to mesenchymal transition

Corresponding Author. Antonio Jimeno M.D., Ph. D., Professor of Medicine/Oncology and Otolaryngology, University of Colorado School of Medicine, 12801 East 17th Avenue, Room L18-8101B, Aurora, CO 80045, Antonio.Jimeno@ucdenver.edu.

Conflict of Interest
All authors in this manuscript declare no conflict of interest

INTRODUCTION

Head and neck squamous cell carcinoma (HNSCC) remains a devastating malignancy with ~50% five-year overall survival (OS) rates (1). During and immediately after treatment a process called accelerated repopulation occurs in HNSCC whereby a few surviving cells rapidly proliferate leading to tumor recurrence (2) but this process still requires elucidation.

One proposed mechanism for how tumor epithelial cells become resistant to therapy is transformation into a more mesenchymal phenotype known as epithelial-to-mesenchymal transition (EMT) (3). Recent reports have linked hedgehog pathway (HhP) signaling to EMT induction following (chemo)radiotherapy in gastric (4, 5), esophageal (6), colorectal (7), ovarian (8) and endometrial (9) cancers. Transcriptional activation of pro-EMT genes by Gli1 can lead to mesenchymal changes (i.e. spindle cell shape, pseudopodia formation) and increased tumor invasiveness. Targeting the HhP or its downstream EMT targets can lead to reversal of the mesenchymal (stem cell "like") phenotype and restoration of chemoradiotherapy sensitivity. A retrospective analysis of RTOG 90-03 demonstrated that HNSCC patients who expressed high levels of Gli1 prior to treatment had poor local control (LC) rates, more distant metastases and worse OS; when correlated with those patients also expressing high levels of epidermal growth factor receptor (EGFR), these patients had the worst outcomes overall (10). We previously demonstrated in HNSCC xenografts that EGFR inhibition leads to up-regulation of the HhP in EGFR-dependent, human papillomavirus (HPV)-negative HNSCC (11). The inter-relatedness of these different pathways suggests that inhibition of both EGFR and the HhP may be necessary to maximize the effectiveness of RT in HNSCC.

The role HhP plays in RT resistance and tumor repopulation in HNSCC remains unknown. We hypothesize that RT similarly modulates the HhP in EGFR-dependent tumors such as HNSCC and could be a mechanism for resistance. Our work examines intra-tumor regional differences in HhP signaling, how RT modulates the HhP, and the effect of HhP inhibition with cyclopamine on HhP gene expression, cell survival, and EMT phenotype in the context of RT. We propose an alternative mechanism where RT-induced Gli1 nuclear (nGLI1) translocation and *GLI1* gene expression is mediated through the mTOR pathway. Lastly, we show that the tumorigenicity of serially co-transplanted tumor and stroma cells increases after radiation and can be abrogated by HhP inhibition.

MATERIAL AND METHODS

Cell Lines and Drugs

HN11 and TU167 HNSCC cell lines have been previously described (11–17). siRNA (AKT, S6K1) was completed in serum free media (SFM) using 1.3μl/ml Dharmafect 1 (Thermo) and 100nM siRNA. *GLI1* silencing was completed using doxycycline-inducible (0.5 μg/ml) pTRIPZ lentiviral constructs (RHS4696-99636732) that introduced small hairpin RNA (shRNA) as previously described (11). Cells were treated with 1μM cyclopamine (LC Laboratories), 1μM Rapamycin (LC Laboratories), or 1μM PF-4708671 (Sigma-Aldrich) for a minimum of 12 hours prior to irradiation. Generation of chronically irradiated cell lines were performed by irradiating cells at 50–60% confluency daily at 2Gy/day for 5 days. Cells

were allowed to recover for 1–2 weeks before initiating the second irradiation cycle. Cells were allowed 1–2 weeks for recovery before initiating any studies.

Irradiation

Cells and animals were irradiated using a RS-2000 (Rad Source Technologies, Inc, GA). Cells were irradiated with 2 or 10Gy using a 160KVp source, at 25mAmp, and at a dose rate of 1.15Gy/min. Mice were irradiated using a customized animal restraint exposing only the head/neck region of the mouse. Radiation dose and dose rate were calculated empirically for the RS-2000.

Colony Formation Assay (CFA)

Serial dilutions were performed and single cells were plated on 6-well plates. Cells were allowed to adhere for 16 hours prior to drug treatment and irradiated with a single dose (0 – 10Gy) at least 8 hours after drug treatment. Cells were washed 3 days after initial drug exposure and grown for an additional 7–10 days until visible colonies on the control plate could be measured. Cells were fixed in 10% formalin solution, stained with 0.5% crystal violet and washed with cold tap water. Threshold for positive proliferative colonies were ≥50 cells. Experiments were replicated either two or three times to generate the RT dose response curves or the RT-cyclopamine cell sensitivity assay curves, respectively.

Human Xenograft Therapeutic Studies

HN11 and TU167 parental cell lines were implanted into athymic nude mice using an established floor-of-the mouth (FOTM) method as previously described (18). 75,000 cells were re-suspended 1:1 in a DMEM/FBS and matrigel mixture and kept on ice until tumor implantation. A 4-arm study was performed to generate efficacy data. Arms used for the parental tumors were: 1) control; 2) cyclopamine 40mg/kg by oral gavage qd for 15 days excluding weekends; 3) RT 5Gy once per week for 3 weeks; or 4) both. When the average tumors reached 100mm^3, mice were distributed into their respective groups. Tumor size was evaluated twice/week using the formula: volume = [length × width^2]/2. For pharmacodynamic analysis on experimental day 10, tumors were extracted 1 hour after drug administration and/or 48 hours after RT and divided into one of two groups: formalin fixation or fluorescence-activated cell sorting (FACS).

We performed a pharmacodynamic study by implanting HNSCC into floor-of-the-mouth and assigning them to one-of-four treatment groups (Supplemental Figure 3A). After receiving the prescribed therapy, tumors were collected from each group, mouse stroma (anti-mouse H2Kd, BioLegend) and human tumor cells (anti-Epcam, Cell Signaling Technology) were separated by FACS, recombined in a 1:3 ratio (5000:15000) with untreated tumor cells, and implanted onto the flanks of athymic nude mice. Tumor regrowth was assessed at 3 and 6 weeks post-implantation and all tumors were excised at 6 weeks for analysis.

Statistics

Two-tailed, Students paired t-test (GraphPad Prism) was used to compare groups for both *in vitro* and *in vivo* experiments. A majority of cell-based experiments were replicated three

times with a minimum of three replicates per experiment. *In vivo* animal experiment statistics were performed on a minimum of 5 animals per group for comparison. Statistical comparisons were performed by group. Statistical values were shown only if p-value were <0.05.

Supplemental Materials and Methods

Additional RNA, protein and immunohistochemical methods are discussed there.

RESULTS

HhP Up-regulation in the Growing Edge of HNSCC Tumors

Utilizing our established patient-derived xenografts (PDX) model system (18), mouse stroma, tumor margin, and tumor center were isolated by laser capture micro-dissection (LCM) from control or irradiated flash-frozen flank tumors (Figure 1A), and evaluated for species-specific *GLI1* expression. In non-irradiated tumors, *hGLI1* at the tumor margin was 4.7× higher compared to the tumor center (P=0.004) (Figure 1B). When comparing irradiated tumor to non-irradiated tumor, normalized *hGLI1* was significantly up-regulated at the margin (8.8×, P=0.02) compared to the center (2.7×, P=0.2). Human sonic hedgehog (SHH), was also significantly up-regulated at the tumor margin by 9.2× in irradiated tumors (P=0.02). Furthermore, *mGli1* demonstrated a non-significant trend towards up-regulation (4.1×) in the mouse stroma (Figure 1C). Results were performed from a single experiment in triplicate. We examined Gli1 expression following RT by immunohistochemistry (IHC) (Figure 1D) at a single time point which demonstrated up-regulation of Gli1 protein but was not differentially increased between the margin and center.

RT Up-regulates the HhP

We used two established human epithelial HPV-negative HNSCC cell lines collected from patients with floor-of-the-mouth (FOTM) SCC (19), HN11 from a primary tumor, and TU167 from a relapsed subject to confirm our *in vivo* observations. We determined whole transcriptome expression differences quantitatively and found dissimilar gene expression levels in the hedgehog, epithelial cell markers, and mTOR pathways (Supplemental Figure 1). Consistent with being a relapsed, more transformed cell type, TU167 had decreased epithelial cell markers, and increased HhP and mTOR pathway expression. Following RT, *GLI1* as well as downstream EMT genes *ZEB2* and *SNAI1* were acutely and significantly up-regulated at 24 and 48 hours (Figure 2A).

EMT is a potential mechanism explaining why LC can be compromised due to accelerated repopulation following prolonged genotoxic stress. We explored whether chronic irradiation modulated HhP and EMT-associated genes. Chronically irradiated HN11 demonstrated up-regulation in HhP (*GLI1*, *GLI2*) and EMT (*ZEB2*, *VIM*) genes compared to the parental line. In TU167, we observed up-regulation of the EMT pathway genes *GLI2* and *TWIST1* (Figure 2B). FACS of chronically irradiated HN11 demonstrated increased VIM expression (~4% of the total population) indicating that a small fraction of these cells have assumed a mesenchymal phenotype (Figure 2C). VIM was higher in parental TU167 compared to HN11, and was not significantly up-regulated by sustained RT.

Effect of Cyclopamine on RT-Mediated GLI1 Up-regulation

To test if RT-induced *GLI1* up-regulation could be suppressed through HhP inhibition, we used the Smoothened receptor inhibitor cyclopamine. Pre-treatment with 1μM cyclopamine followed by RT significantly suppressed RT-induced *GLI1* in HN11 but not in TU167 (Figure 3A). Using shGLI1, we documented partial *GLI1* suppression in HN11 but not in TU167 following RT (Supplemental Figure 2). Cells pre-treated with 1μM cyclopamine demonstrated no significant change in nGLI1 content at 1, 2, and 4 hours. Despite inhibition with cyclopamine, we still observed a two-fold increase in nGli1 in HN11 and TU167 (Figure 3B, first and third panels) following RT. Similarly, cytoplasmic Gli1 (cGli1) was similarly increased following irradiation and suppressed with cyclopamine pretreatment. Interestingly, cGli1 levels were unable to be fully suppressed following irradiation despite pre-treatment with cyclopamine. This effect was more pronounced in TU167 compared to HN11 (Figure 3B, second and fourth panels). Treating with higher (but not clinically achievable) concentrations of cyclopamine (10μM) led to significant inhibition of RT-induced *GLI1* expression suggesting a dose-response effect (data not shown).

Using CFA's, the primary cell line HN11 was significantly more radiosensitive than TU167 at lower RT doses (Figure 3C). We then evaluated whether cyclopamine inhibition could enhance cytotoxicity at single radiation dose. Combinatorial therapy with cyclopamine+RT demonstrated a significant effect compared to single modality therapy or no treatment (control vs 1μM+RT: TU167, P=0.003; HN11, P=0.0006) with the greatest response seen in HN11 (Figure 3D) compared to TU167 (Figure 3E). Chronically irradiated HN11 cells exposed to 1μM cyclopamine for 12 hours demonstrated a trend towards suppressing *GLI1* (1.7±0.3 to 1.5±0.2, n.s.), *GLI2* (1.7±0.03 to 1.1±0.02, P=0.0025), and *VIM* (3.0±0.2 to 1.1±0.1, P=0.0043). No trend was observed for TU167 for *GLI1*, *GLI2* or *VIM*. These findings demonstrated that chronically irradiated HN11 cells that induce HhP and EMT-associated genes were responsive to cyclopamine inhibition.

In vivo Effect of RT and Cyclopamine in an Orthotopic HNSCC Model

To further our *in vitro* observations, we evaluated tumors *in vivo* combining cyclopamine and RT. Mice were implanted in the FOTM (Figure 4A) with either HN11 or TU167 cell lines and randomized to one of 4 treatment arms (Figure 4B). RT±cyclopamine led to a reduction in tumor volume compared to control or cyclopamine alone in HN11 and TU167 parental tumors (Figure 4C, 4D). Of note, cyclopamine had no effect on inhibiting tumor growth in HN11, although, similar to the control arm continued to grow. It has not been reported in the literature that cyclopamine stimulates tumor proliferation and given the size of the error bar compared to the control arm, is unlikely to be suggestive of the above hypothesis. In HN11, tumor volumes responded dramatically to RT (67% reduction) or the combination treatment (77% reduction), which correlated well with their *in vitro* susceptibility to RT (Figure 4C). In TU167, we observed smaller tumor sizes in both the RT alone and combinatorial therapy arms (RT: 37% reduction compared to control; cyclopamine+RT: 49% reduction compared to control) (Figure 4D). TU167 irradiated tumors had a propensity for developing cystic, cavitated lesions (RT: 3/10 tumors; dual therapy: 8/10) (Supplemental Figure 3A) beginning around day 25. At day 45, representative cystic and non-cystic TU167 tumors were harvested from euthanized mice for analysis. The

non-cystic tumors by H/E were solid throughout compared to the cystic tumors, which were only a thin rim of tissue (Supplemental Figure 3B). Tumor proliferation evaluated using Ki67 for the non-cystic tumors revealed that control (H-score:80) or cyclopamine-treated (H-score:80) tumors demonstrated the highest amount of Ki67 staining compared to RT (H-score:65) or dual therapy-treated (H-score:40) tumors. The dual therapy-treated tumors demonstrated the most reduced Ki67 staining both in the periphery and core (Supplemental Figure 3C). This suggests that there was both increased necrosis and decreased proliferation in RT and dual treated TU167 tumors, in spite of small volumetric differences. In comparison, the cystic versus non-cystic RT treatment tumors suggest less proliferating cells in the cystic tumors and growth is restricted to the tumor margin/edge.

Tumors were harvested for pharmacodynamic analysis 10 days into treatment and IHC staining performed for EGFR, Gli1, ALDH1, and BMI1. EGFR staining confirmed presence of HNSCC cells over mouse stroma. Faint Gli1 expression was observed in control cells and this was significantly up-regulated throughout the tumor following RT. RT-induced Gli1 expression could be partially abrogated by cyclopamine treatment (Figure 5, HN11 (Left) and TU167) (Right). When evaluating the mouse stroma, we similarly observed an increase in stromal Gli1 following RT and a pronounced decrease with dual therapy by H-score. In particular, we observed a pronounced effect with cyclopamine alone in suppressing mouse stromal GLI1 in TU167 over HN11 (Supplemental Table 1). Similarly, ALDH1 and BMI1 were up-regulated following RT and partially inhibited by cyclopamine.

Given our *in vitro* and *in vivo* findings, we next sought to explore: 1) an alternative mechanism which may drive tumor Gli1 cytoplasmic-to-nuclear translocation independent of the canonical HhP and 2) whether inhibition of HhP in stromal cells can block tumor repopulation *in vivo*.

mTOR/S6K1 Mediates GLI1 Cytoplasmic-to-Nuclear Translocation

In both cell lines, despite inhibition with significant concentrations of cyclopamine, RT was still able to induce *GLI1* gene expression and increase nGli1 accumulation suggesting that an accessory pathway (independent of canonical HhP signaling) may be driving RT-induced nGli1 accumulation. Therefore, we hypothesized that RT could activate the mTOR/S6K1 pathway and enhance Gli1 cytoplasmic-to-nuclear translocation (Figure 6A). Following RT, *GLI1* was up-regulated by 24 hours in both HN11 and TU167 (Figure 6B), and pre-treatment with 1μM ZSTK474 (AKT inhibitor) was able to significantly suppress *GLI1* expression in HN11 following RT but not in TU167 (data not shown). This resistance was consistent with the observed over-expression of the mTOR pathway in TU167, and use of a more specific inhibitor was warranted. Following pre-treatment with 1μM rapamycin, we observed suppression of both *GLI1* mRNA and Gli1 cytoplasmic-to-nuclear protein accumulation following RT in TU167 (Figure 6C). We observe a similar increase in cGli1 following irradiation and the irradiation effect can similarly be suppressed with rapamycin pretreatment. In contrast, HN11 inhibition with rapamycin did not prevent RT-induced nGli1 accumulation (Supplemental Figure 4) and is in contrast to our mRNA results. Our transcriptome results may offer an answer for this discrepancy where TU167 has greater mTOR gene expression compared to HN11 and may be more sensitive to the effects of

mTOR inhibition which may translate into dimished Gli1 accumulation. Cellular Gli1 content is known to be regulated both at the transcriptional and proteasomal level (20). The suppression of *GLI1* may suggest that rapamycin's role may be to regulate gene expression and perhaps is irrespective of nuclear protein accumulation.

Next we evaluated whether inhibition of the downstream mTOR effector S6K1 could prevent nGli1 accumulation. Similarly, *GLI1* expression was significantly reduced in the presence of S6K1 inhibitor (1μM PF-4708671) following RT (Figure 6B). We attempted to determine whether loss of S6K1 could similarly suppress *GLI1* expression and prevent nuclear Gli1protein accumulation. Four siRNA constructs were screened and their ability to suppress S6K1 expression by mRNA and immunoblot were assessed. The two best candidate constructs were then selected. Both siRNA constructs suppressed expression of S6K1. ppS6K1 was still observed despite knock-down and was completely absent following RT. Our results suggest that inhibition with one siRNA construct was able to suppress nGli1 accumulation in both HN11 and TU167. However, the other siRNA construct gave contrary results and does not appear to suppress RT-induced Gli1 nuclear accumulation (Supplemental Figure 5). Our findings suggest a possible link between mTOR/S6K1 and nGli1 accumulation but must be interpreted with caution.

In Vivo Tumor Repopulation Following RT

Loco-regional failure due to tumor repopulation following RT or chemoradiotherapy remains a significant problem. *In vitro* and *in vivo* studies have implicated that genotoxically-stressed tumor or fibroblast cells may play a role in tumor repopulation. *In vivo*, tumor and tumor-associated fibroblasts (stroma) are closely admixed with one another. Based on our patient-derived xenograft and TU167 *in vivo* results demonstrating increased mouse stromal Gli1 following RT, subsequent suppression by pre-treatment with cyclopamine and the significant response of TU167 tumors to dual therapy, we hypothesized that cyclopamine may also target the tumor stroma and given its combined affect on TU167 *in vivo*, may inhibit tumor repopulation. We treated orthotopically implanted TU167 tumors with vehicle, cyclopamine, RT, or the combination, surgically resected them, separated tumor and stroma compartments by flow cytometry, and co-implanted these in different permutations with untreated tumor cells (Supplemental Figure 6A). This addressed whether the irradiated tumor or stroma could enhance tumor repopulation and whether inhibition of the HhP could abrogate repopulation. We observed a significant 10-fold difference in tumor regrowth at 3 weeks favoring the irradiated stroma combined with fresh tumor cell lines (S_{RT}:T) compared to the non-irradiated control stroma:tumor (S_C:T) pairing (P=0.01). When stroma cells pre-treated with cyclopamine and RT were combined with fresh tumor (S_D:T), we observed a significant reduction in tumor regrowth rates at 3 weeks when S_D:T was compared against S_{RT}:T (P=0.007) implicating that HhP following RT may be involved in stroma-mediated tumor repopulation (Figure 7A). We also evaluated T_{RT}:T pairings and observed a similar though non-significant trend in tumor regrowth at 3 weeks. (Figure 7A, Supplemental Table 2). When we evaluated the same pairings between S_{RT}:T versus T_{RT}:T, there was greater than a four-fold difference in size favoring the S_{RT}:T over the tumor:tumor pairing (P=0.03) (Supplemental Table 2). Figure 7B shows representative mice with S:T and T:T pairings at 6 weeks. At 6 weeks, the T_{RT}:T pairings continued to demonstrate a

significant trend towards smaller tumor sizes (267±27 mm^3 versus 579±102 mm^3) compared to the S_{RT}:T pairings (P=0.05). Representative excised tumors from all animals continued to demonstrate that S_{RT} cells conferred a significant growth advantage over S_C or S_{Cyc} (non-RT) stroma. Furthermore, tumors pretreated with cyclopamine were able to inhibit tumor regrowth despite being irradiated (Figure 7A and C).

DISCUSSION

RT remains the cornerstone for local management of HNSCC either definitively or in the post-operative setting. Whether RT can induce GLI1/HhP up-regulation through an EMT phenotype as a mechanism for tumor repopulation, and the respective relevance of irradiated cancer cells versus intra-tumor stromal cells for tumor repopulation remain unknown. Accelerated tumor repopulation following RT is associated with loco-regional recurrence in patients and a better understanding of this mechanism is critical to improve LC and OS.

The interface between tumor margin/edge and tumor stroma is an important distinction for cancer biology. First, we demonstrated that *GLI1* is significantly upregulated at the tumor edge compared to the core in non-irradiated samples. Secondly, following RT, *GLI1* gene expression was up-regulated at the peripheral tumor edge compared to the tumor core. Of note, this was taken at a solitary time point (48 hours post-RT) and even though overall Gli1 content has increased in both cells there is no observed preference for staining at the tumor edge. Based on this experiment, accumulation of nGli1 preferentially at the tumor edge may occur more rapidly as our immunoblot results suggest and therefore tumor harvested at an earlier time point might illustrate this.

The implications of our findings are important since tumors with up-regulated Gli1 and/or the EMT pathway have been shown to be more chemo- and radioresistant, more locally invasive, and metastatic (7, 21–23). Secondly, the peripheral tumor cells model those cell islands left behind after surgical resection (“positive margin”). This is clinically significant since a positive margin indicates a high risk for recurrence and patients with positive margins often experience greater local and distant failure rates when they fail to receive adequate doses of RT/chemoradiotherapy (24, 25). The change in tumor milieu, increased inflammation, and local hypoxia following surgery may provide additional factors that allow a high Gli1 expressing tumor more opportunity to proliferate/flourish compared to a low Gli1 expressing tumor. Our results demonstrated that *GLI1* expression is inherently higher at the tumor margin compared to the core, and that RT can further induce *GLI1* overexpression at the tumor margin. However, these findings need to be cautiously interpreted and we caveat that tumor heterogeneity may cause variations in gene expression between tumor margin and center and this may explain the more uniform Gli1 protein expression following irradiation observed by IHC as compared to the qRT-PCR results which demonstrated greater *GLI1* expression at the tumor margin. Another explanation is that RT leads to *GLI1* up regulation which in turn up regulates certain EMT associated genes. A limited number of these cells which are more EMT-like can transform to a more mesenchymal phenotype and settle in to the existing environment or translocate away from the source of insult (ie. local RT). As they are away from the area of insult, these cells can down regulate various mesenchymal genes and re-establish their epithelial phenotype (mesenchymal-to-epithelial

phenotype) allowing them to grow in a new microenvironment. This has been illustrated in a squamous cell epithelial cancer model using a conditional doxycycline regulatory system controlling *TWIST1* expression (26). The authors demonstrated that *TWIST1* expression was necessary for EMT but shutting down *TWIST1* was necessary for establishing distant metastasis. This explanation takes into account both the tumor margin and heterogeneity issues providing a possible mechanism for Gli1 mediated treatment failure and distant metastasis.

In the chronically irradiated cells, we observed that HhP genes, *GLI1* and *GLI2*, and EMT genes, *ZEB2*, *TWIST1* and *VIM*, were up-regulated though not as robustly as when cells were acutely irradiated. These genes remained elevated 2–8 weeks following RT suggesting that a surviving population of irradiated cancer cells adapt gene expression allowing for survival and repopulation. Other groups including our own have demonstrated that inhibition of HhP or EMT pathway genes, *TWIST*, *SNAI1* or *SLUG*, can reverse (chemo)-RT resistance and decrease tumor invasiveness, progression, and metastasis (8, 9, 11, 22, 27). Therefore, we decided to evaluate whether HhP inhibition could enhance tumor control by either increasing radiosensitivity or preventing tumor repopulation *in vivo*. A recent paper indicated that inadequate RT doses in other tumor cell lines can lead to increased tumor regrowth mediated by the HhP (21). Therefore, direct inhibition of Gli1 activation *in vivo* may lead to enhanced tumoricidal effects when combined with RT. When we treated our chronically irradiated HN11 cells with cyclopamine, down regulation of *GLI2* and *VIM* occurred, indicating that HhP inhibition in HNC may be an appropriate anti-cancer target when combined with RT.

Our IHC results demonstrated that Gli1 is up-regulated in both tumors and in the tumor stroma following RT and this up-regulation was mitigated with cyclopamine. Interestingly, the downstream stem cell marker and DNA damage response protein ALDH1 and BMI1, respectively, were both downregulated following cyclopamine therapy suggesting that these genes are regulated by Gli1 and that HhP inhibition may prevent or slow the transition to a more "stem-cell like" state. In one study evaluating patients with high versus low ALDH1 expression pre- and post-surgery, colorectal cancer patients undergoing neoadjuvant chemoradiotherapy who expressed high levels of ALDH1 had greater rates of local failure and recurrence (28). Expression of ALDH1 in HNSCC and colorectal cancer is associated with increased nodal and distant metastasis, worse OS, and is mediated through *TWIST1* and *SNAI1* expression (29, 30). These findings highlight the concern that chemoradiotherapy can induce *ALDH1* (and *BMI1*) expression which is a poor prognostic factor. Our results are the first to demonstrate that adding cyclopamine to RT can suppress Gli1 expression in HPV-negative HNC and thereby down-regulate ALDH1 and BMI1 expression *in vivo*.

Accelerated tumor repopulation following RT is a well-known phenomenon but its mechanism remains unknown. Our *in vitro* results suggest that both HN11 and TU167 up-regulate the HhP acutely and chronically following RT. Furthermore, cyclopamine can suppress RT-induced *GLI1* in HN11 but not in TU167 despite our *in vivo* results, and this is likely due to lower baseline levels of HhP expression in HN11 compared to TU167. Given the difference in our *in vitro* versus our *in vivo* data, this led us to question if an alternative target may be the stroma. Our own LCM qRT-PCR and IHC results (Figure 1C, 4E) show

the mouse stroma also up-regulated *GLI1* following RT but that *GLI1* is suppressed following cyclopamine treatment. One possible explanation is that irradiated stroma may provide a nurturing environment to allow circulating mesenchymal tumor cells a nidus to grow. Researchers have demonstrate that irradiated fibroblasts undergo changes including matrix remodeling (ie. release of MMP's) and cytokine release (ie. TGF-beta, basic FGF). This may allow for an altered albeit rich growth environment allowing tumor cells to flourish. A growing body of literature in prostate, breast, pancreas and other cancers suggests that HhP up-regulation in the tumor microenvironment through paracrine signaling plays a substantial role in tumor growth, survival, angiogenesis and metastasis (27, 31–34). More specifically, cancer associated fibroblasts (CAFs) have been shown to upregulate both the Smoothened receptor and in turn *GLI1* (35) and *SNAI1* (36) while another group demonstrated inhibition of Smoothened on CAFs in turn translated to decreased *GLI1* expression and the downstream EMT gene *SNAI1* in pancreatic cancer cells (37) supporting a paracrine signaling model for EMT. These findings indicate that both stromal and tumor Gli1 may play an important role in tumor treatment resistance and repopulation and targeting them may not only enhance CAF sensitivity to genotoxic agents but also inhibit the EMT process in tumors.

Building on our findings, we hypothesized that the HhP may play a role in the HPV negative tumor microenvironment and tumor repopulation following RT. When we irradiated stroma and recombined them with fresh tumor cells, it resulted in significant rapid tumor regrowth after re-implantation compared to control or cyclopamine alone. Compared to the irradiated tumor recombined with fresh tumor cells, we observed a non-significant trend at 3 weeks and a more pronounced regrowth effect at 6 weeks. Interestingly, we did not see substantial tumor regrowth in the irradiated stroma (or tumors) treated with cyclopamine when combined with fresh tumor at either timepoint. Our findings are novel as they implicate Gli1 as a potential target in the stromal microenvironment important for RT-induced HNSCC tumor (re)growth. However, additional work is needed to understand what may be driving this regrowth but our findings suggest that HhP may be involved. Since the tumor microenvironment decisively contributes to therapy resistance (38), modulating its signaling through targeted therapy may enhance LC rates. Our findings suggest that irradiated HPV negative HNSCC stroma (and to a lesser degree, irradiated HNSCC tumor) utilize the HhP to mediate tumor repopulation. Identifying the paracrine signaling molecule(s) interacting with the tumor stroma will provide valuable information regarding tumor biology which could be applied towards novel drug discovery. There is a distinct lack of information regarding HPV positive HNSCC and the HhP in the literature. Given their excellent response to traditional chemoradiotherapy, we would hypothesize that the HhP may not play as important a role but this will need to be addressed with formal experimentation.

Our observation that *GLI1* and EMT-associated genes and proteins can be similarly up-regulated following acute or chronic irradiation implicates their importance as radio-responsive genes. Our transcriptome analysis of TU167 showed that it was less epithelial compared to HN11 and had greater gene enrichment for the Hedgehog and mTOR pathways. Higher basal expression of HhP genes in TU167 may explain its relative insensitivity to cyclopamine *in vitro* but this was overcome with higher doses of drug. In

esophageal cancer, TNFα has been shown to activate/stabilize Gli1 via mTOR/S6K1 and not through the canonical Smoothened pathway (6). Furthermore, RT, either through EGFR phosphorylation (39) or directly through DNA damage response proteins such as DNA-PKcs (40), has been shown to activate the PI3K/AKT/mTOR pathway. Our pharmacologic findings suggest that RT-induced nGli1 translocation may signal through the mTOR/S6K1 pathway in more mesenchymal appearing cell lines such as TU167 and may be the primary driver for RT-induced nGli1 accumulation. However, in more epithelial cell lines such as HN11, rapamycin was unable to suppress nGli1 accumulation yet *GLI1* mRNA remained suppressed following pharmacologic inhibition. One possible explanation is that rapamycin may affect *GLI1* expression irrespective of nuclear accumulation. One hypothesis is that mesenchymal versus epithelial cells likely signal differently upstream but converge through mTOR/S6K1. Others have similarly demonstrated that the mTOR pathway is upregulated in HNC and may be an attractive clinical target. One group has shown that rapamycin combined with an AKT inhibitor, enzastaurin, can decrease survival, angiogenesis, and proliferation in preclinical HNC models (41). Furthermore, two Phase I clinical studies have been completed: the first in resected, locally advanced HNC patients combining everolimus, weekly cisplatin and radiation and the second, combining everolimus with docetaxel and cisplatin as part of an induction chemotherapy regimen. Both clinical studies have demonstrated tolerability and safety and are presumed to be progressing to Phase II (42, 43). It is enticing to consider that the combination of an mTOR inhibitor, cyclopamine, and RT in recurrent or locally-advanced HNC patients may be more efficacious since it targets both the tumor and stroma-mediated components involved with tumor repopulation.

Our results show that the HhP and Gli1 play an important role in HNSCC tumor biology. We have demonstrated that the mTOR/S6K1 pathway may contribute to RT-induced Gli1 signaling *in vitro*. RT combined with targeting HhP led to increased HNSCC cytotoxicity *in vitro* and *in vivo* and limited tumor repopulation *in vivo*. In locally recurrent or metastatic head-neck tumors that may be mTOR driven, combining mTOR and HhP inhibitors with RT may allow an opportunity to target primary and alternative mechanisms including stroma signaling which may lead to improved therapeutic efficacy.

Supplementary Material

Refer to Web version on PubMed Central for supplementary material.

Acknowledgments

Support

Supported by 1R01CA149456 (A.J.), R21DE019712 (A.J.), 2012 Cancer League of Colorado Grant (G.N.G., A.J.), 2013 ASTRO Resident/Fellow Research Seed Grant # RA2013-1 (G.N.G., A.J.), T32CA174648 (P.N.L), National Institutes of Health Cancer Center Support Grant P30 CA046934, and the Paul Wehling Fund.

References

1. Siegel R, Naishadham D, Jemal A. Cancer statistics, 2013. CA Cancer J Clin. 2013; 63:11–30. [PubMed: 23335087]
2. Hall, E.; Giaccia, A. Radiobiology for the Radiologist. 7th ed.. Philadelphia: Lippincott Williams and Wilkins; 2012.

3. Polyak K, Weinberg RA. Transitions between epithelial and mesenchymal states: acquisition of malignant and stem cell traits. Nat Rev Cancer. 2009; 9:265–273. [PubMed: 19262571]
4. Ohta H, Aoyagi K, Fukaya M, Danjoh I, Ohta A, Isohata N, et al. Cross talk between hedgehog and epithelial-mesenchymal transition pathways in gastric pit cells and in diffuse-type gastric cancers. Br J Cancer. 2009; 100:389–398. [PubMed: 19107131]
5. Isohata N, Aoyagi K, Mabuchi T, Daiko H, Fukaya M, Ohta H, et al. Hedgehog and epithelial-mesenchymal transition signaling in normal and malignant epithelial cells of the esophagus. Int J Cancer. 2009; 125:1212–1221. [PubMed: 19431210]
6. Wang Y, Ding Q, Yen CJ, Xia W, Izzo JG, Lang JY, et al. The crosstalk of mTOR/S6K1 and Hedgehog pathways. Cancer Cell. 2012; 21:374–387. [PubMed: 22439934]
7. Kawamoto A, Yokoe T, Tanaka K, Saigusa S, Toiyama Y, Yasuda H, et al. Radiation induces epithelial-mesenchymal transition in colorectal cancer cells. Oncol Rep. 2012; 27:51–57. [PubMed: 21971767]
8. Kurrey NK, Jalgaonkar SP, Joglekar AV, Ghanate AD, Chaskar PD, Doiphode RY, et al. Snail and slug mediate radioresistance and chemoresistance by antagonizing p53-mediated apoptosis and acquiring a stem-like phenotype in ovarian cancer cells. Stem Cells. 2009; 27:2059–2068. [PubMed: 19544473]
9. Tsukamoto H, Shibata K, Kajiyama H, Terauchi M, Nawa A, Kikkawa F. Irradiation-induced epithelial-mesenchymal transition (EMT) related to invasive potential in endometrial carcinoma cells. Gynecol Oncol. 2007; 107:500–504. [PubMed: 17905419]
10. Chung CH, Dignam JJ, Hammond ME, Klimowicz AC, Petrillo SK, Magliocco A, et al. Glioma-associated oncogene family zinc finger 1 expression and metastasis in patients with head and neck squamous cell carcinoma treated with radiation therapy (RTOG 9003). J Clin Oncol. 2011; 29:1326–1334. [PubMed: 21357786]
11. Keysar SB, Le PN, Anderson RT, Morton JJ, Bowles DW, Paylor JJ, et al. Hedgehog Signaling Alters Reliance on EGF Receptor Signaling and Mediates Anti-EGFR Therapeutic Resistance in Head and Neck Cancer. Cancer Res. 2013; 73:3381–3392. [PubMed: 23576557]
12. Jimeno A, Kulesza P, Kincaid E, Bouaroud N, Chan A, Forastiere A, et al. C-fos assessment as a marker of anti-epidermal growth factor receptor effect. Cancer Res. 2006; 66:2385–2390. [PubMed: 16489045]
13. Yonesaka K, Zejnullahu K, Lindeman N, Homes AJ, Jackman DM, Zhao F, et al. Autocrine production of amphiregulin predicts sensitivity to both gefitinib and cetuximab in EGFR wild-type cancers. Clin Cancer Res. 2008; 14:6963–6973. [PubMed: 18980991]
14. Amador ML, Oppenheimer D, Perea S, Maitra A, Cusatis G, Iacobuzio-Donahue C, et al. An epidermal growth factor receptor intron 1 polymorphism mediates response to epidermal growth factor receptor inhibitors. Cancer Res. 2004; 64:9139–9143. [PubMed: 15604284]
15. Frederick MJ, Holton PR, Hudson M, Wang M, Clayman GL. Expression of apoptosis-related genes in human head and neck squamous cell carcinomas undergoing p53-mediated programmed cell death. Clin Cancer Res. 1999; 5:361–369. [PubMed: 10037186]
16. Frederick BA, Helfrich BA, Coldren CD, Zheng D, Chan D, Bunn PA Jr, et al. Epithelial to mesenchymal transition predicts gefitinib resistance in cell lines of head and neck squamous cell carcinoma and non-small cell lung carcinoma. Mol Cancer Ther. 2007; 6:1683–1691. [PubMed: 17541031]
17. Rangan SR. A new human cell line (FaDu) from a hypopharyngeal carcinoma. Cancer. 1972; 29:117–121. [PubMed: 4332311]
18. Keysar SB, Astling DP, Anderson RT, Vogler BW, Bowles DW, Morton JJ, et al. A patient tumor transplant model of squamous cell cancer identifies PI3K inhibitors as candidate therapeutics in defined molecular bins. Mol Oncol. 2013; 7:776–790. [PubMed: 23607916]
19. Zhao M, Sano D, Pickering CR, Jasser SA, Henderson YC, Clayman GL, et al. Assembly and initial characterization of a panel of 85 genomically validated cell lines from diverse head and neck tumor sites. Clin Cancer Res. 2011; 17:7248–7264. [PubMed: 21868764]
20. Huntzicker EG, Estay IS, Zhen H, Lokteva LA, Jackson PK, Oro AE. Dual degradation signals control Gli protein stability and tumor formation. Genes Dev. 2006; 20:276–281. [PubMed: 16421275]

21. Ma J, Tian L, Cheng J, Chen Z, Xu B, Wang L, et al. Sonic hedgehog signaling pathway supports cancer cell growth during cancer radiotherapy. PLoS One. 2013; 8:e65032. [PubMed: 23762282]
22. Feldmann G, Dhara S, Fendrich V, Bedja D, Beaty R, Mullendore M, et al. Blockade of hedgehog signaling inhibits pancreatic cancer invasion and metastases: a new paradigm for combination therapy in solid cancers. Cancer Res. 2007; 67:2187–2196. [PubMed: 17332349]
23. Sims-Mourtada J, Izzo JG, Apisarnthanarax S, Wu TT, Malhotra U, Luthra R, et al. Hedgehog: an attribute to tumor regrowth after chemoradiotherapy and a target to improve radiation response. Clin Cancer Res. 2006; 12:6565–6572. [PubMed: 17085672]
24. Bernier J, Domenge C, Ozsahin M, Matuszewska K, Lefebvre JL, Greiner RH, et al. Postoperative irradiation with or without concomitant chemotherapy for locally advanced head and neck cancer. N Engl J Med. 2004; 350:1945–1952. [PubMed: 15128894]
25. Cooper JS, Pajak TF, Forastiere AA, Jacobs J, Campbell BH, Saxman SB, et al. Postoperative concurrent radiotherapy and chemotherapy for high-risk squamous-cell carcinoma of the head and neck. N Engl J Med. 2004; 350:1937–1944. [PubMed: 15128893]
26. Tsai JH, Donaher JL, Murphy DA, Chau S, Yang J. Spatiotemporal regulation of epithelial-mesenchymal transition is essential for squamous cell carcinoma metastasis. Cancer Cell. 2012; 22:725–736. [PubMed: 23201165]
27. Zeng J, Aziz K, Chettiar ST, Aftab BT, Armour M, Gajula R, et al. Hedgehog Pathway Inhibition Radiosensitizes Non-Small Cell Lung Cancers. Int J Radiat Oncol Biol Phys. 2013; 86:143–149. [PubMed: 23182391]
28. Deng Y, Zhou J, Fang L, Cai Y, Ke J, Xie X, et al. ALDH1 is an independent prognostic factor for patients with stages II-III rectal cancer after receiving radiochemotherapy. Br J Cancer. 2014; 110:430–434. [PubMed: 24327017]
29. Huang CF, Xu XR, Wu TF, Sun ZJ, Zhang WF. Correlation of ALDH1, CD44, OCT4 and SOX2 in tongue squamous cell carcinoma and their association with disease progression and prognosis. J Oral Pathol Med. 2014; 43:492–498. [PubMed: 24450601]
30. Kim YH, Kim G, Kwon CI, Kim JW, Park PW, Hahm KB. TWIST1 and SNAI1 as markers of poor prognosis in human colorectal cancer are associated with the expression of ALDH1 and TGF-beta1. Oncol Rep. 2014; 31:1380–1388. [PubMed: 24402192]
31. Fingas CD, Bronk SF, Werneburg NW, Mott JL, Guicciardi ME, Cazanave SC, et al. Myofibroblast-derived PDGF-BB promotes Hedgehog survival signaling in cholangiocarcinoma cells. Hepatology. 2011; 54:2076–2088. [PubMed: 22038837]
32. Harris LG, Pannell LK, Singh S, Samant RS, Shevde LA. Increased vascularity and spontaneous metastasis of breast cancer by hedgehog signaling mediated upregulation of cyr61. Oncogene. 2012; 31:3370–3380. [PubMed: 22056874]
33. Mills LD, Zhang Y, Marler RJ, Herreros-Villanueva M, Zhang L, Almada LL, et al. Loss of the Transcription Factor GLI1 Identifies a Signaling Network in the Tumor Microenvironment Mediating KRAS-Induced Transformation. J Biol Chem. 2013; 288:11786–11794. [PubMed: 23482563]
34. Levina E, Chen M, Carkner R, Shtutman M, Buttyan R. Paracrine Hedgehog increases the steroidogenic potential of prostate stromal cells in a Gli-dependent manner. Prostate. 2012; 72:817–824. [PubMed: 22025366]
35. Walter K, Omura N, Hong SM, Griffith M, Vincent A, Borges M, et al. Overexpression of smoothened activates the sonic hedgehog signaling pathway in pancreatic cancer-associated fibroblasts. Clin Cancer Res. 2010; 16:1781–1789. [PubMed: 20215540]
36. Choe C, Shin YS, Kim SH, Jeon MJ, Choi SJ, Lee J, et al. Tumor-stromal interactions with direct cell contacts enhance motility of non-small cell lung cancer cells through the hedgehog signaling pathway. Anticancer Res. 2013; 33:3715–3723. [PubMed: 24023301]
37. Hwang RF, Moore TT, Hattersley MM, Scarpitti M, Yang B, Devereaux E, et al. Inhibition of the hedgehog pathway targets the tumor-associated stroma in pancreatic cancer. Mol Cancer Res. 2012; 10:1147–1157. [PubMed: 22859707]
38. Sun Y, Campisi J, Higano C, Beer TM, Porter P, Coleman I, et al. Treatment-induced damage to the tumor microenvironment promotes prostate cancer therapy resistance through WNT16B. Nat Med. 2012; 18:1359–1368. [PubMed: 22863786]

39. Pickhard AC, Margraf J, Knopf A, Stark T, Piontek G, Beck C, et al. Inhibition of radiation induced migration of human head and neck squamous cell carcinoma cells by blocking of EGF receptor pathways. BMC Cancer. 2011; 11:388. [PubMed: 21896192]

40. Boehme KA, Kulikov R, Blattner C. p53 stabilization in response to DNA damage requires Akt/PKB and DNA-PK. Proc Natl Acad Sci U S A. 2008; 105:7785–7790. [PubMed: 18505846]

41. Liu J, Kuo WL, Seiwert TY, Lingen M, Ciaccio MF, Jones RB, et al. Effect of complementary pathway blockade on efficacy of combination enzastaurin and rapamycin. Head Neck. 2011; 33:1774–1782. [PubMed: 21438065]

42. Fury MG, Lee NY, Sherman E, Ho AL, Rao S, Heguy A, et al. A phase 1 study of everolimus + weekly cisplatin + intensity modulated radiation therapy in head-and-neck cancer. Int J Radiat Oncol Biol Phys. 2013; 87:479–486. [PubMed: 24074921]

43. Fury MG, Sherman E, Ho AL, Xiao H, Tsai F, Nwankwo O, et al. A phase 1 study of everolimus plus docetaxel plus cisplatin as induction chemotherapy for patients with locally and/or regionally advanced head and neck cancer. Cancer. 2013; 119:1823–1831. [PubMed: 23408298]

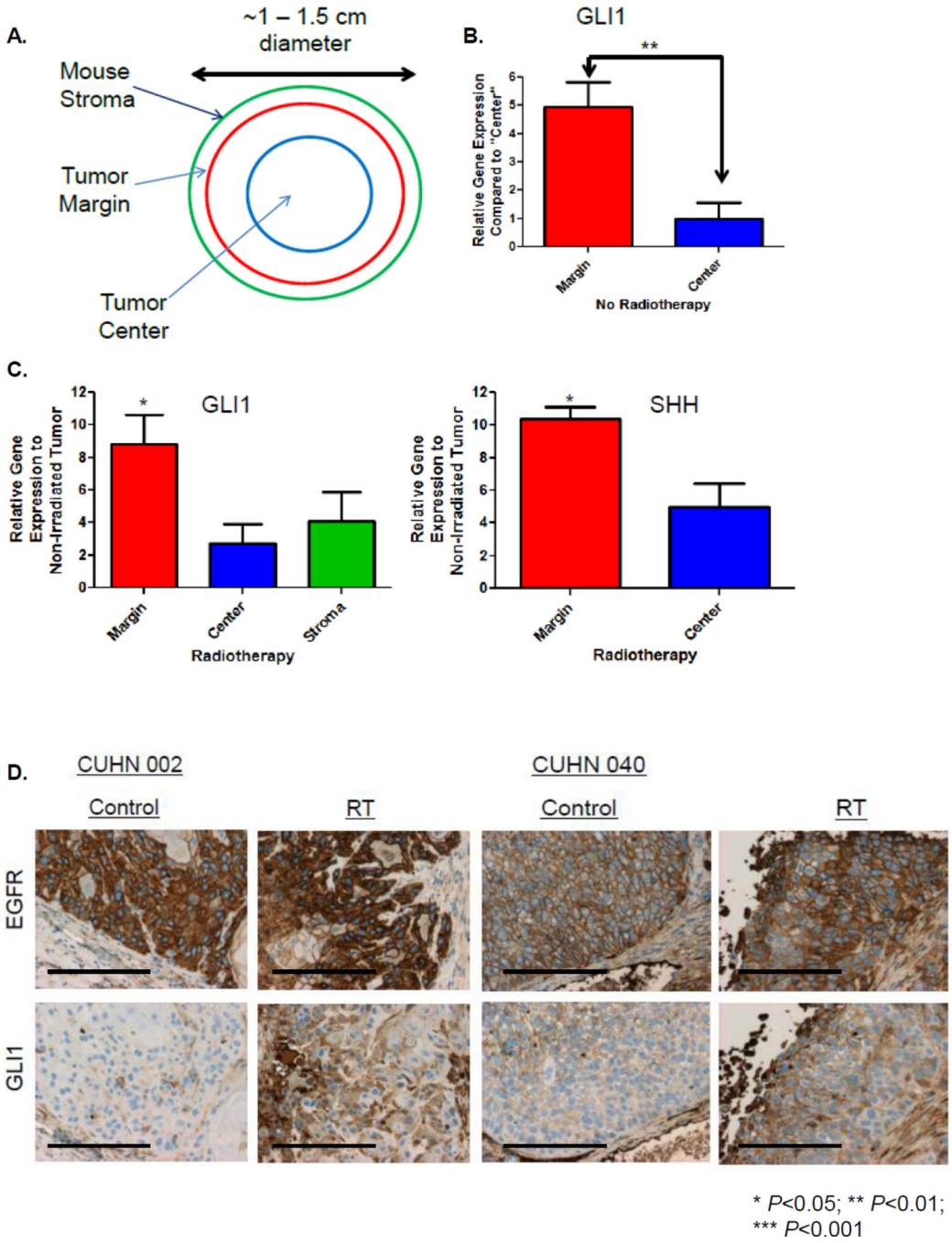

Figure 1. RT Induces *GLI1* Expression *In Vivo*

A. Schema describing tumor sections of interest that were laser capture microdissected (LCM). **B**. The amount of non-irradiated human *GLI1* mRNA expression at the tumor margin compared to the tumor center was determined by quantitative real-time PCR (qRT-PCR) from LCM tissue. **C**. Irradiated and non-irradiated LCM tissue was analyzed by qRT-PCR using species specific probes for *GLI1* and *SHH* to determine RT-induced gene fold expression over baseline. **D.** Two different PDX±RT. Tumors were harvested, formalin

fixed, sectioned and stained with anti-EGFR or anti-Gli1 for IHC (20×, bar 100μM). Statistically significant findings were denoted: *P<0.05.

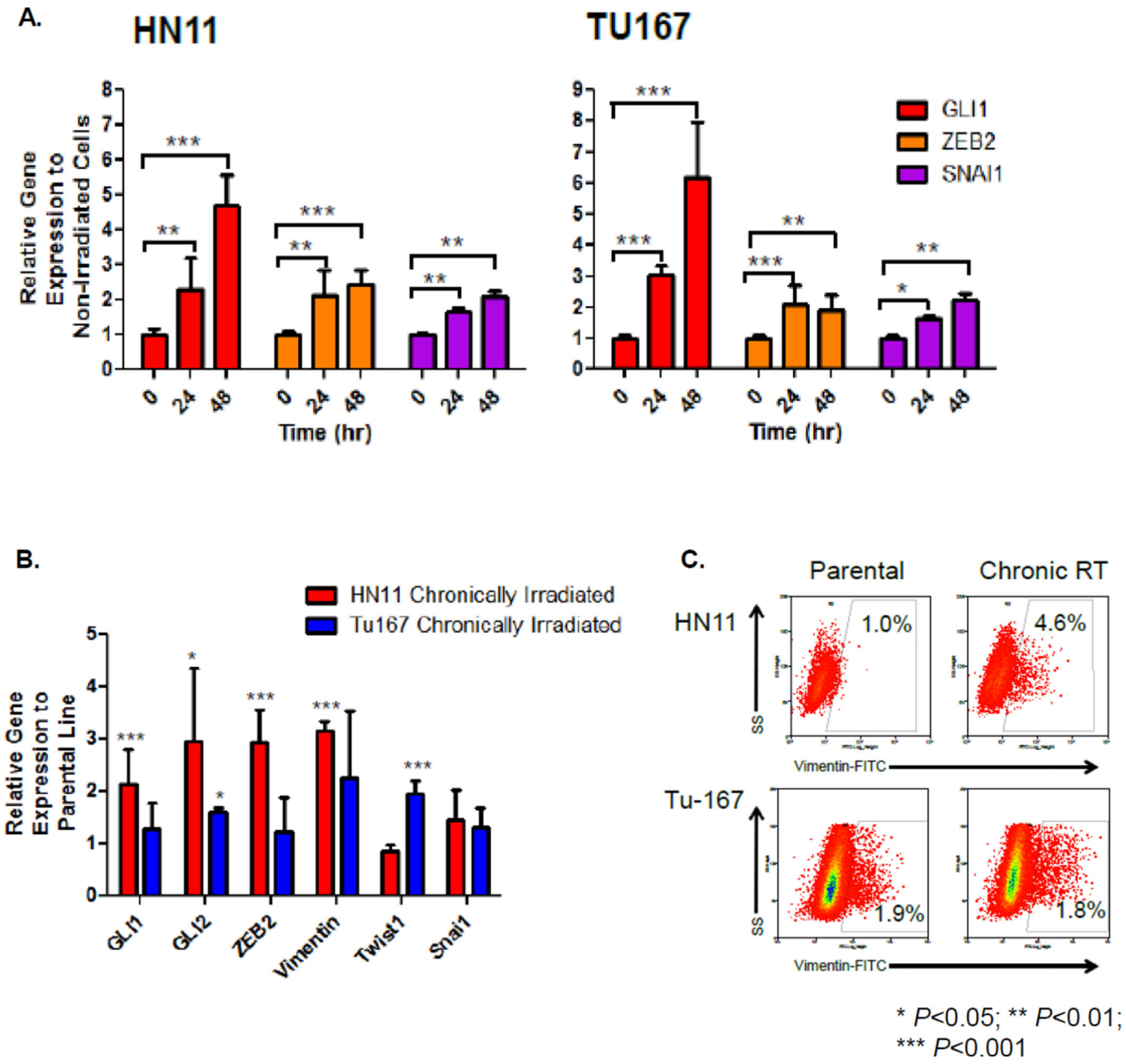

Figure 2. RT Induces *In Vitro* GLI1 Expression

A. Mechanistic studies were performed on two HNSCC cell lines: TU167, HN11. *GLI1, ZEB2, SNAI1* expression was evaluated by qRT-PCR at 0, 24 and 48 hours. **B.** Chronically irradiated cells compared to their original parental cell lines were evaluated for HhP or EMT-gene expression by qRT-PCR. **C.** Expression levels of Vim were evaluated between parental and chronically irradiated cells by FACS. Statistically significant findings were denoted: *P<0.05; **P<0.01; ***P< 0.001.

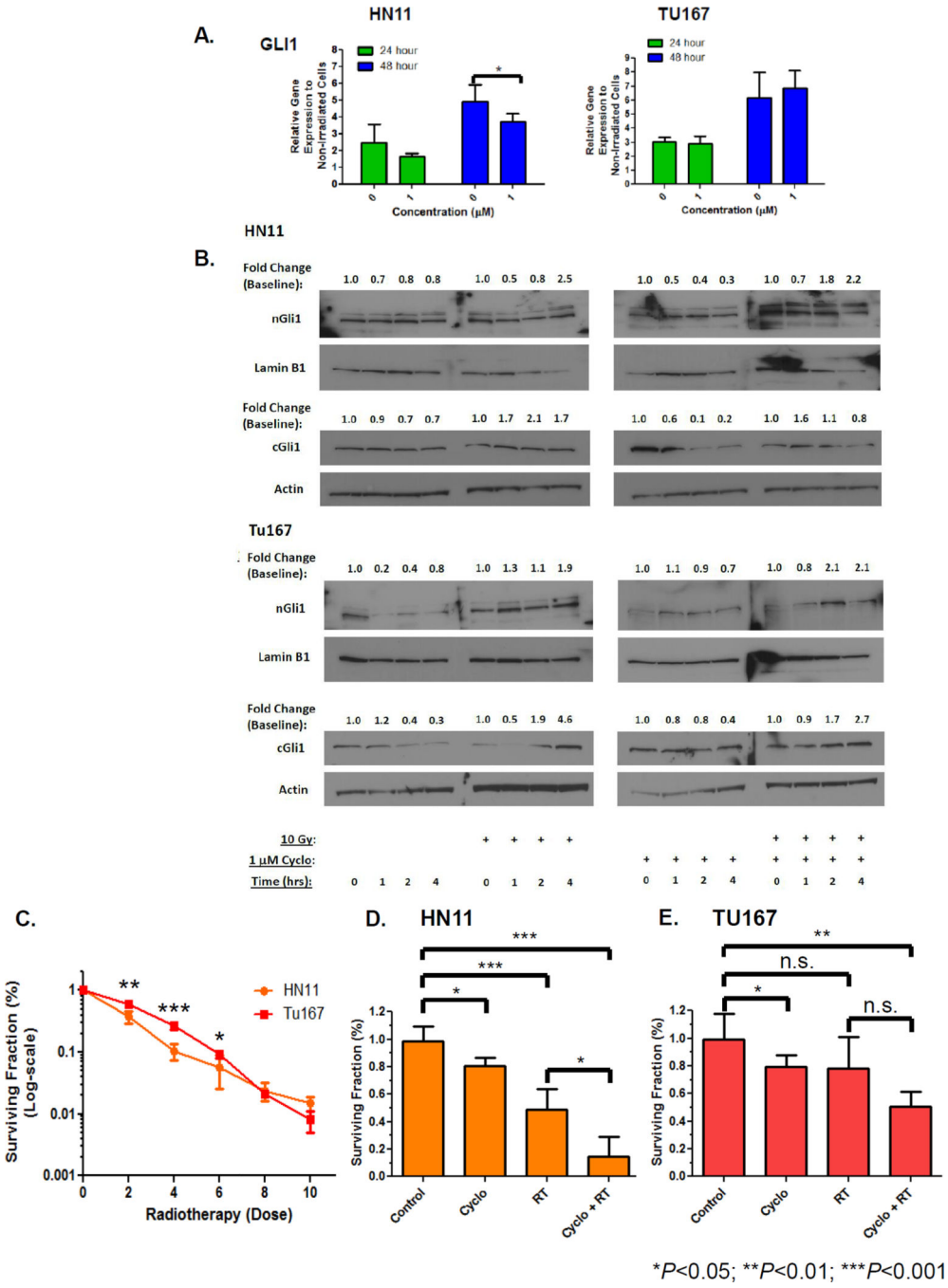

Figure 3. Effect of Cyclopamine on RT Induced *GLI1* Gene Expression and Cytotoxicity

A. Cells were pretreated with 1μM cyclopamine 8 hours prior to receiving RT. Cells were harvested at specific time points and *GLI1* expression evaluated by qRT-PCR. **B**. Nuclear extracts were generated as previous described from cells ±1μM cyclopamine ±RT. nGLI1 accumulation was evaluated by immunoblot and temporal fold changes described. **C.** CFA RT dose curves were generated from serially diluted cells grown on 6-well plates treated 24 hours after adhesion with 0–10Gy irradiation. Cells were fixed, stained and counted ~8–10 days after RT. CFA's were performed to assess the effect of cyclopamine and 2Gy RT on

cell growth and survival on HN11 (**D**) and TU167 (**E**). Eight hours prior to irradiation, cells were pre-treated with 1μM cyclopamine in low serum media (LSM). LSM was chosen as it more closely represents the tumor milieu. Furthermore, use of LSM prior to drug treatment will prevent exogenous growth factors from competing with the effects of cyclopamine. Statistically significant findings were denoted: **P*<0.05; ***P*<0.01; ****P*< 0.001.

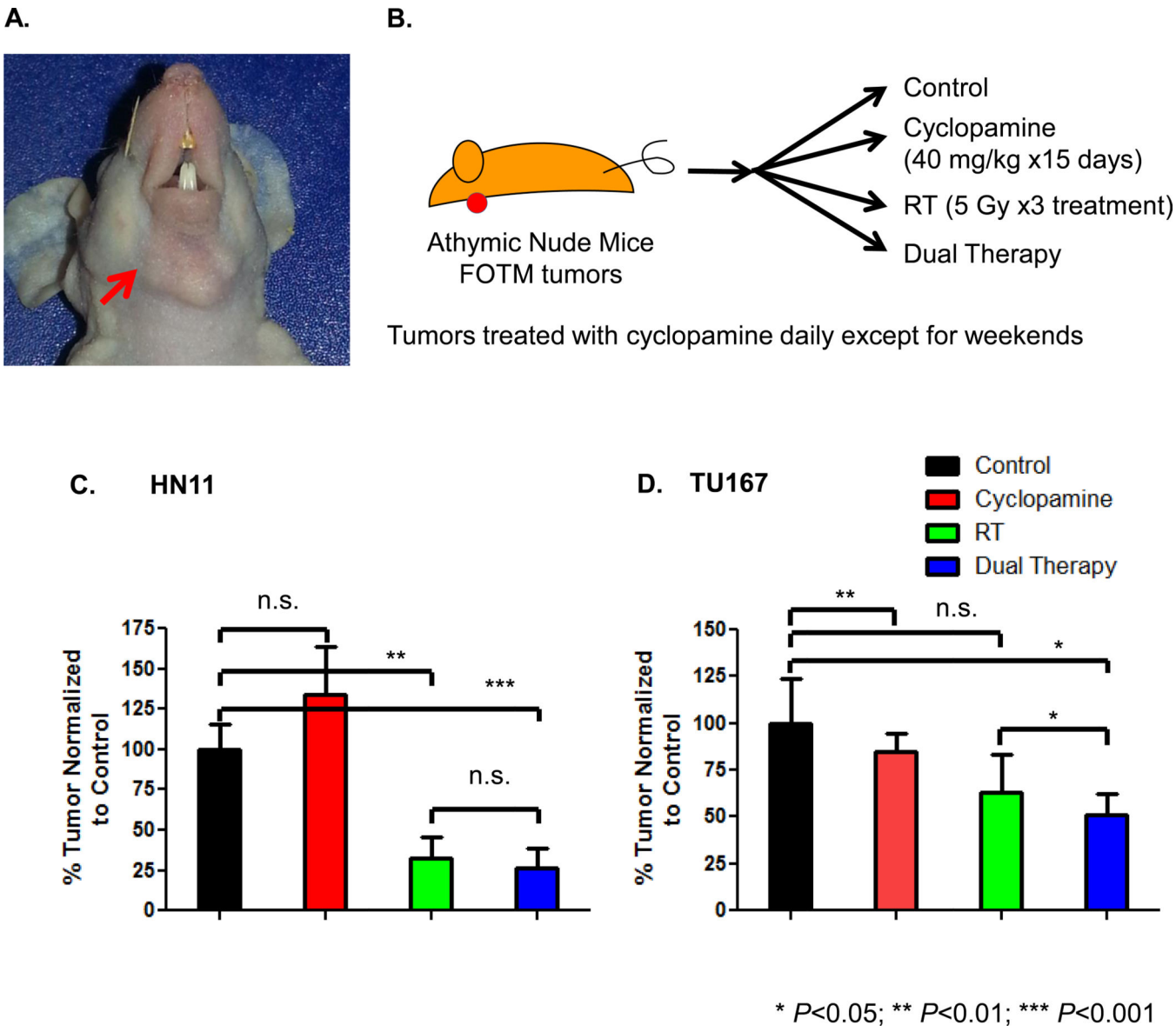

Figure 4. *In Vivo* Effects of Cyclopamine and RT

A. Figure describing location of orthotopic FOTM tumor implanted in athymic nude mouse.

B. Schema describing cyclopamine and/or RT dose and duration for animal tumor growth studies. Tumor growth for orthotopically implanted FOTM HN11 (**C**) and TU167 (**D**) parental tumors was assessed at 28 days post-treatment initiation.

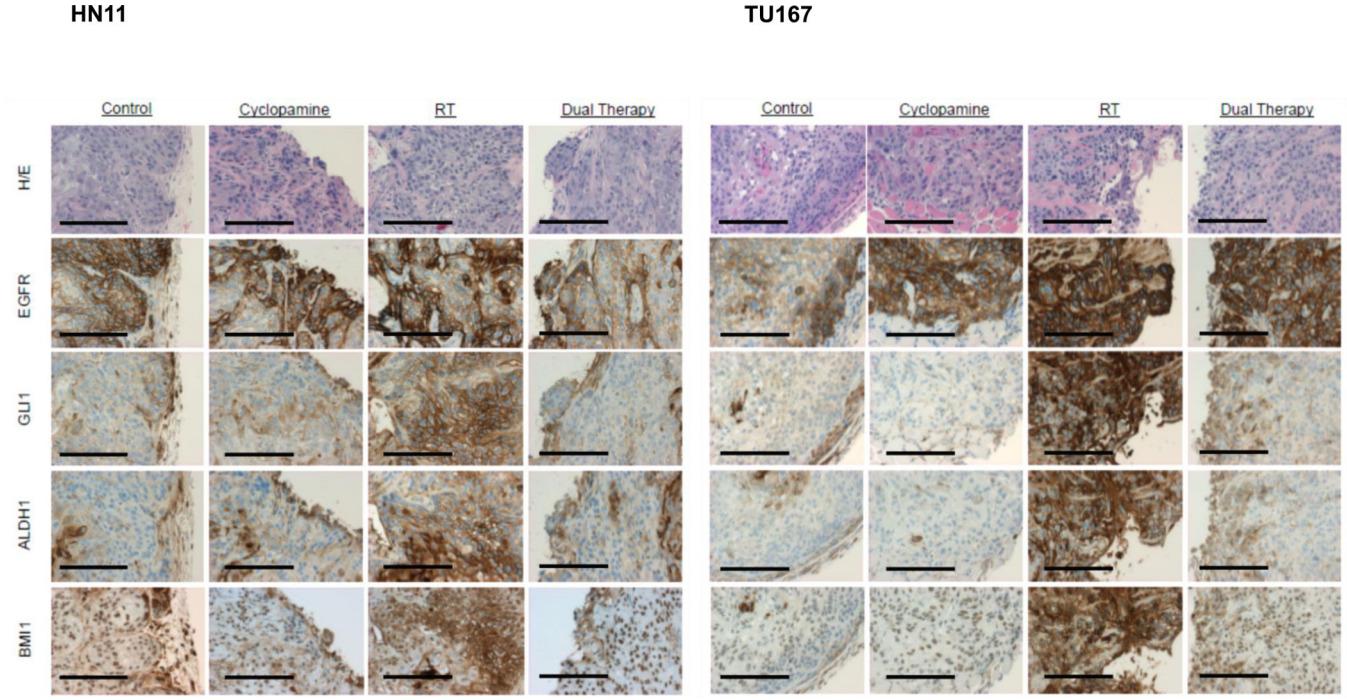

Figure 5. RT-Induced GLI1, ALDH1, BMI1 Expression

IHC was performed on formalin-fixed tumors and stained with either H/E, EGFR, GLI1, ALDH1, or BMI1. Differences in IHC (20×, bar 100μM) expression were evaluated by H-score.

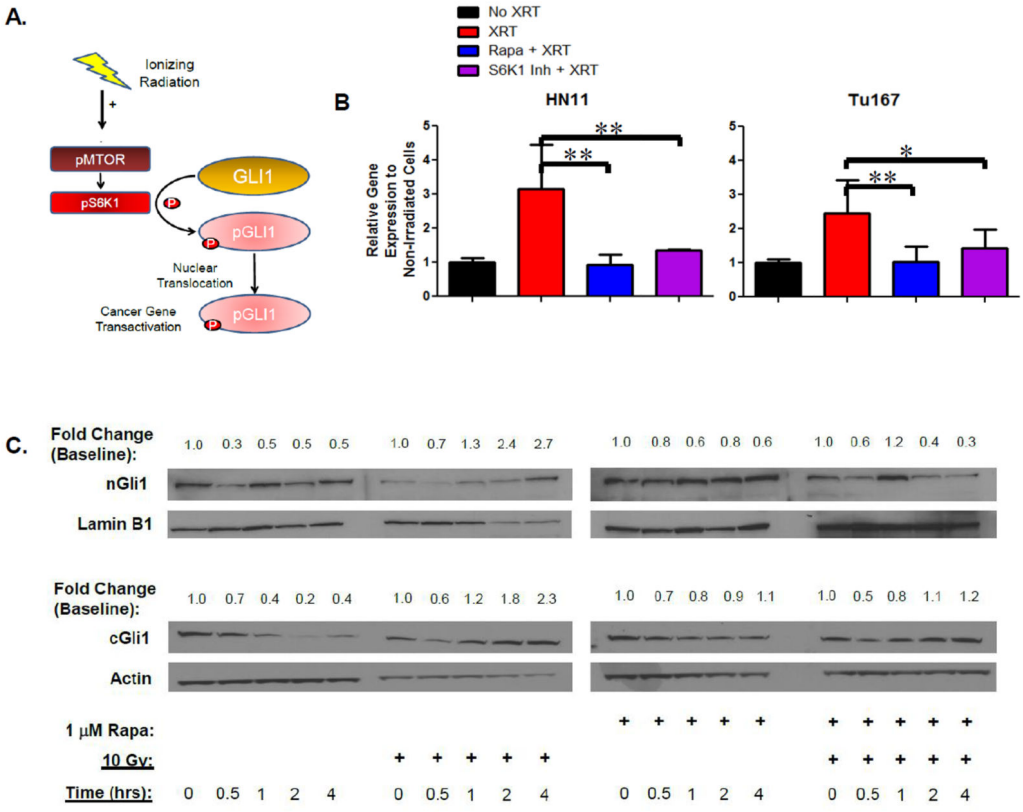

* $P<0.05$; ** $P<0.01$; *** $P<0.001$

Figure 6. RT-Induced Mechanism for Nuclear GLI1 Accumulation

A. Schema proposing a mechanism for RT mediated GLI1 cytoplasmic-to-nuclear translocation. **B.** Targeted inhibitors against mTOR and S6K1 were used on cells pretreated with drug 12 hours before RT to determine if *GLI1* gene expression could be inhibited. Cells were harvested 24 hours following irradiation and *GLI1* gene expression analyzed by qRT-PCR. **C.** Cytoplasmic and nuclear extracts were generated as previous described from TU167 treated with ±1μM rapamycin ±RT. cGli1 and nGli1 accumulation was evaluated by

immunoblot and temporal fold change were described. Statistically significant findings were denoted: *P<0.05; **P<0.01.

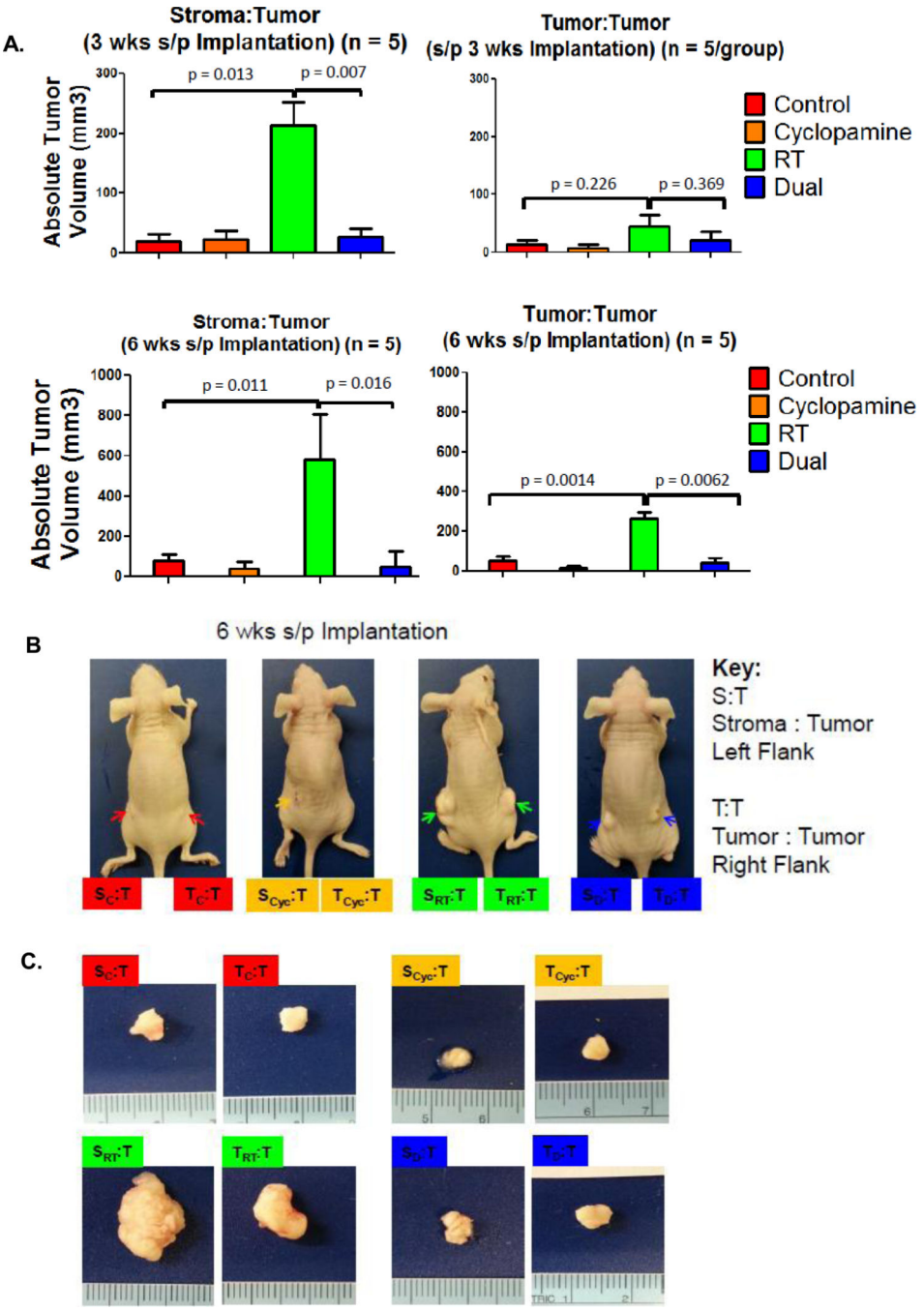

Figure 7. Effect of RT on *In Vivo* Tumor Repopulation in TU167

A. All potential flank tumors were measured at 3 (Top) and 6 (Bottom) weeks post-implantation. Stromal:tumor (S:T) and tumor:tumor (T:T) combinations were implanted on the left and right flanks, respectively. **B.** Labels: Red, Orange, Green, Blue corresponds to pre-treatment control, cyclopamine, RT and dual therapy groups. At 6 weeks post-implantation, final measurements were taken and tumors harvested for analysis. **C.**

Representative excised tumors are shown for each of the four pre-treatment arms with corresponding left and right flank tumors for the two different groups.